ISSN 1063-7788, Physics of Atomic Nuclei, 2015, Vol. 78, No. 4, pp. 509–520. © Pleiades Publishing, Ltd., 2015.
Original Russian Text © S.V. Shmatov, 2015, published in Yadernaya Fizika, 2015, Vol. 78, No. 6, pp. 546–557.

ELEMENTARY PARTICLES AND FIELDS
Experiment

Overview of Physics Results from the CMS Experiment at the LHC

S. V. Shmatov*

Joint Institute for Nuclear Research, ul. Joliot-Curie 6, Dubna, Moscow oblast, 141980 Russia

Received December 1, 2014

Abstract—An overview of physics results from the CMS experiment at the LHC is given. The present analysis is based on data obtained for colliding proton beams at the c.m. energies of $\sqrt{s} = 7$ and 8 TeV over the period spanning 2011 and 2012. Results from proton–nucleus and nucleus–nucleus runs are also given.

DOI: 10.1134/S1063778815030114

1. INTRODUCTION

The Compact Muon Solenoid (CMS) experiment [1] is one of the two multipurpose experiments intended for implementation in proton and nuclear beams of the Large Hadron Collider (LHC).

Predictions of the Standard Model (SM) of particle interactions proved to be highly compelling and astoundingly precise. Despite this and despite the discovery of the its last cornerstone—that is, the Higgs boson [2]—the Standard Model is not complete: specifically, it is unable to explain cosmological observations of dark matter and the matter–antimatter asymmetry in the Universe. Solving these problems requires invoking symmetry groups broader than that underlying the Standard Model or radically new theoretical concepts. Systematic searches for signals predicted by various extensions of the Standard Model are among the main tasks of the CMS experiment. The experiment is intended for detecting a broad spectrum of particles produced in proton–proton and heavy-ion interactions. The CMS studies properties of known particles at previously inaccessible energy scales and performs searches for new unpredicted phenomena [3, 4]. A complete description of the CMS detector systems and their physical and technical features is given in [1].

An overview of basic results from the CMS experiment that were obtained in colliding proton and nuclear beams over the first cycle of LHC operation from 2010 to 2012 is given in the present article. The investigations of the CMS experiment were based on data of 2011 at the c.m. collision energy of $\sqrt{s} = 7$ TeV and data of 2012 at the c.m. collision energy of $\sqrt{s} = 8$ TeV. The size of the data sample under analysis corresponded to the integrated luminosity of 5.1 fb^{-1} in 2011 and the integrated luminosity of 20.1 fb^{-1} in 2012.

2. STANDARD MODEL PHYSICS

2.1. QCD Processes

Investigation of the multiparticle production of charged hadrons began almost immediately after the commissioning of the LHC at 2009. This was done first at the c.m. energy of $\sqrt{s} = 0.9$ TeV and then at the c.m. energies of $\sqrt{s} = 2.36$ and 7 TeV [5]. A substantial deviation of the resulting multiplicity distributions (see Fig. 1*a*) and the differential rapidity density as a function of the c.m. collision energy (see Fig. 1*b*) for charged particles from predictions of theoretical models was revealed. This required tuning the parameters of codes for simulations of physics events in order to interpret further new data from the LHC.

Measurement of cross sections for inclusive jet production revealed good agreement between data reported in [6] and Standard Model predictions in the next-to-leading-order (NLO) approximation of perturbative QCD at jet transverse momenta in the region extending up to 2 TeV/c. An analysis of double jet production—that is, measurement of the respective differential cross sections $d\sigma/dM_{jj}$ in the invariant-mass region extending up to 5 TeV/c^2 [7] and of the angular distributions of jets [8]—did not reveal deviations from theoretical expectations either but made it possible to establish boundaries of parameters of physics scenarios beyond the Standard Model (for more details, see Section 4).

A comparison of cross sections for the production of two and three jets revealed good agreement between data and Standard Model predictions for values of the total transverse momentum H_T between

*E-mail: Sergei.Shmatov@cern.ch

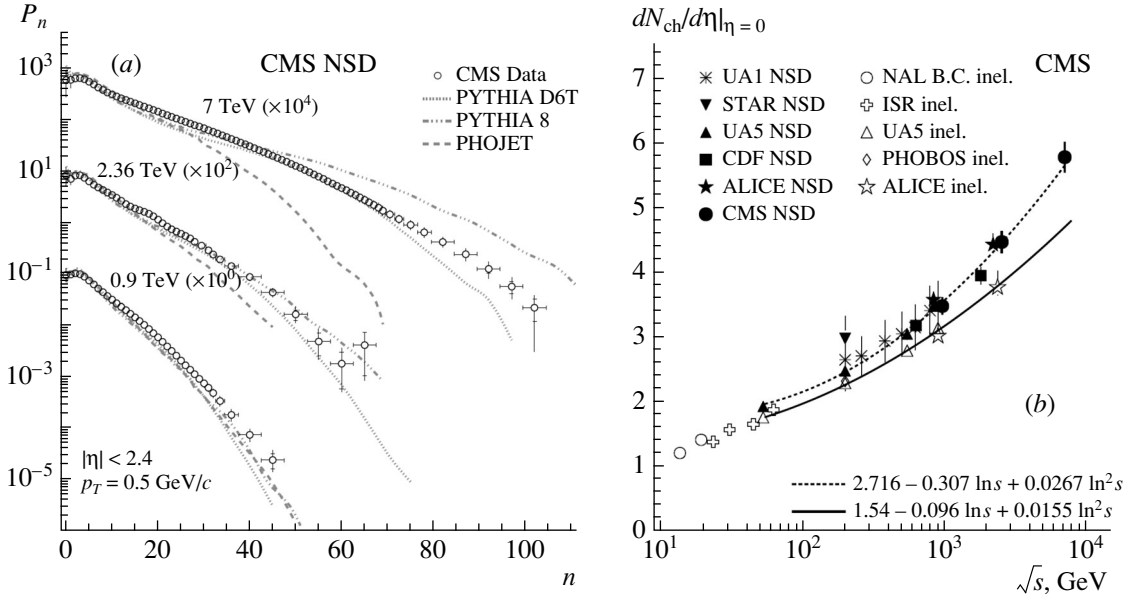

Fig. 1. (*a*) Multiplicity distributions of charged hadrons and (*b*) differential rapidity density of the event multiplicity as a function of the c.m. collision energy $\sqrt{s}$.

0.5 and 5 TeV/c and made it possible to extract for the first time the value of the QCD running coupling constant, $\alpha_s(M_Z) = 0.1148 \pm 0.0014(\text{expt.}) \pm 0.0018(\text{PDF}) \pm 0.0050(\text{theor.})$, in the jet-transverse-momentum region around $p_T^{\text{jet}} \sim 1$ TeV/c [9]. Later on, this value was refined on the basis of data on inclusive jet production at p_T^{jet} of up to 3 TeV/c: $\alpha_s(M_Z) = 0.1185 \pm 0.0019(\text{expt}) \pm 0.0028(\text{PDF}) \pm 0.0004(\text{theor})$ [10]. These data were also used to test various quark and gluon distribution functions.

2.2. Electroweak Processes

Measurements of the total cross sections for the production of W and Z gauge bosons and the branching ratios for their decays through various channels at $\sqrt{s} = 7$ and 8 TeV became one the first results obtained at the LHC in studying electroweak processes [11, 12]. At $\sqrt{s} = 8$ TeV, the measured values of the cross sections multiplied by the respective branching ratios were $\sigma(pp \to WX) \times \text{Br}(W \to l\nu) = 11.9 \pm 0.03(\text{stat.}) \pm 0.22(\text{syst.}) \pm 0.52(\text{lum.})$ nb and $\sigma(pp \to ZX) \times \text{Br}(Z \to l^+l^-) = 1.12 \pm 0.01(\text{stat.}) \pm 0.02(\text{syst.}) \pm 0.05(\text{lum.})$ nb [12]. As the size of the accumulated data sample grew, it became possible to measure rarer processes like the associated production of $W/Z/\gamma$ and several jets (Fig. 2*a*) [13] and the production of gauge-boson pairs [14, 15]. The results obtained in this way showed close agreement with Standard Model predictions. Also, theoretical predictions obtained in the next-to-next-to-leading order (NNLO) of perturbation theory complied with the experimentally measured differential ($d\sigma/dM$) and double-differential ($d^2\sigma/dMdY$) cross sections for Drell–Yan processes in the dielectron and dimuon channels [16]. Measurements of spatial [17, 18] and charged asymmetries and values of the effective Weinberg angle [18, 19] did not reveal deviations from Standard Model predictions either.

Measurements of the top-quark mass were performed in channels featuring leptons and jets, the dilepton channel, and the hadron channel. The value obtained by combining data from the ATLAS and CMS experiments [20], $m_t = 173.29 \pm 0.23(\text{stat.}) \pm 0.26(\text{syst.})$ GeV/c^2, is in good agreement with data from experiments at the Tevatron, $m_t = 173.20 \pm 0.51(\text{stat.}) \pm 0.36(\text{syst.})$ GeV/c^2 [21]. The accuracy of the measurements was not poorer than 1%.

Measurements of the cross sections for single and double top-quark production were performed simultaneously with this. The cross-section value of $\sigma_{t\bar{t}} = 165.8 \pm 2.2(\text{stat.}) \pm 13.2(\text{syst.}) \pm 6.1(\text{syst.})$ pb at $\sqrt{s} = 7$ TeV [22] is in good agreement with the Standard Model value of $\sigma_{t\bar{t}} = 167^{+17}_{-18}$ pb. These results formed a basis for the first determination of the QCD running coupling constant. The resulting value of $\alpha_s(M_Z) = 0.1178^{+0.0046}_{-0.0040}$ complies to a high degree of precision with the world-average value. The measured cross-section value of $\sigma_{t\bar{t}} = 239 \pm 2(\text{stat.}) \pm 11(\text{syst.}) \pm 6(\text{lum.})$ pb at $\sqrt{s} = 8$ TeV [23]

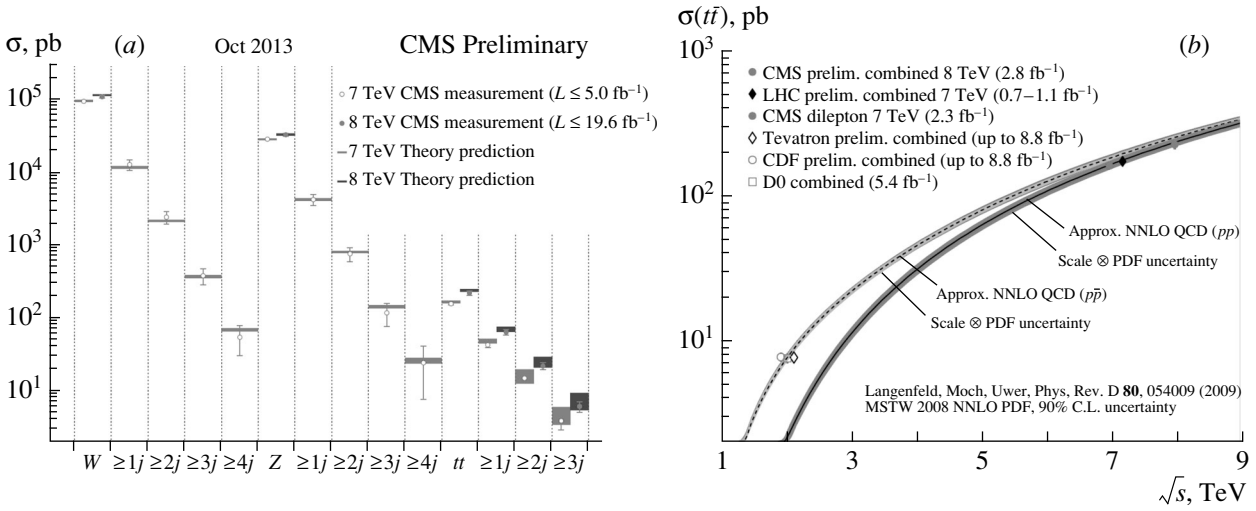

Fig. 2. (*a*) Cross section for the associated production of gauge bosons and jets. (*b*) Cross section for the production of t-quark pairs as a function of $\sqrt{s}$. Shown in the figure are the results of experiments at the LHC and Tevatron along with the NNLO theoretical predictions with respective uncertainties (shaded regions around the curves).

also showed agreement with Standard Model predictions at $m_t = 172.5\ \text{GeV}/c^2$ (Fig. 2*b*).

The total cross sections for single top-quark production at $\sqrt{s} = 7$ and 8 TeV [24, 25] and the cross sections for the associated production of a top quark and a W boson [26], as well as the corresponding differential cross sections with respect to the mass, rapidity, and momentum transfer were measured in the t and s channels. The results are in perfect agreement with theoretical expectations. The measured results for the top-quark polarization, $P_n = 0.009 \pm 0.029 \pm 0.041$ [27], and for the helicity asymmetry, $A_{\text{helicity}} = 0.24 \pm 0.02(\text{стат.}) \pm 0.08(\text{syst.})$ [28], agree with the respective Standard Model predictions.

Rare Standard Model processes that escaped detection in previous experiments were studied for the first time in the CMS experiment. The associated production of a single top quark and a W boson was observed on the basis of a data sample that corresponded to the integrated luminosity of $\mathcal{L}_{\text{int}} = 12.2\ \text{fb}^{-1}$ [29]. The measured reaction cross section of $\sigma_{tW} = 23.4 \pm 5.4$ pb proved to be in perfect agreement with the Standard Model Prediction. This cross-section value was used to calculate the matrix element $|V_{tb}|$. The result was $|V_{tb}| = 1.03 \pm 0.12(\text{expt}) \pm 0.04(\text{theor})$.

2.3. Rare Decays

The decays of B mesons (which consist of one b quark and a light quark) to two muons provide a perfect method for indirectly observing physics beyond the Standard Model. The decays of B mesons of different types—B_0 consisting of b and d quarks and B_s consisting of b and s quarks—to muon pairs are strongly suppressed in the Standard Model. Some extensions of the Standard Model predict either a substantial enhancement or a still stronger suppression of these decays. Anyway, a deviation of measured decay branching ratios from respective Standard Model predictions would be a clear-cut signal of new physics beyond the Standard Model. For more than 25 years, many experiments have been aimed at searches for these rare decays. Over this time, the sensitivity limits have been improved by four orders of magnitude. Now, they approach the value predicted by the Standard Model. For the first time, the observation of the decay $B_s \to \mu\mu$ was reliably demonstrated by the LHCb experiment in November 2012 with a statistical significance of 3.2σ [30].

Experimental data collected in 2011 and 2012 at the integrated luminosities of $\mathcal{L}_{\text{int}} = 4.9$ and $20.4\ \text{fb}^{-1}$, respectively, were used by the CMS Collaboration for this purpose. The excess of the number of events of the decay $B_s \to \mu\mu$ above the background in the invariant-mass distribution of dimuons (Fig. 3*a*) made it possible to estimate the branching ratio for this decay at $(3.0^{+1.0}_{-0.9}) \times 10^{-9}$ with allowance for the systematic and statistical uncertainties [31]. The statistical significance of this observation was 4.3σ. The result of the CMS measurement for the decay $B_s \to \mu\mu$ agrees with the value of $(3.6 \pm 3) \times 10^{-9}$ predicted for the branching ratio by the Standard Model. This demonstrates compellingly the validity of Standard Model predictions. Also, searches for the decay $B_0 \to \mu\mu$ were performed; as a result, a limit below which the decay in question was not found was determined for its branching ratio. This limit is

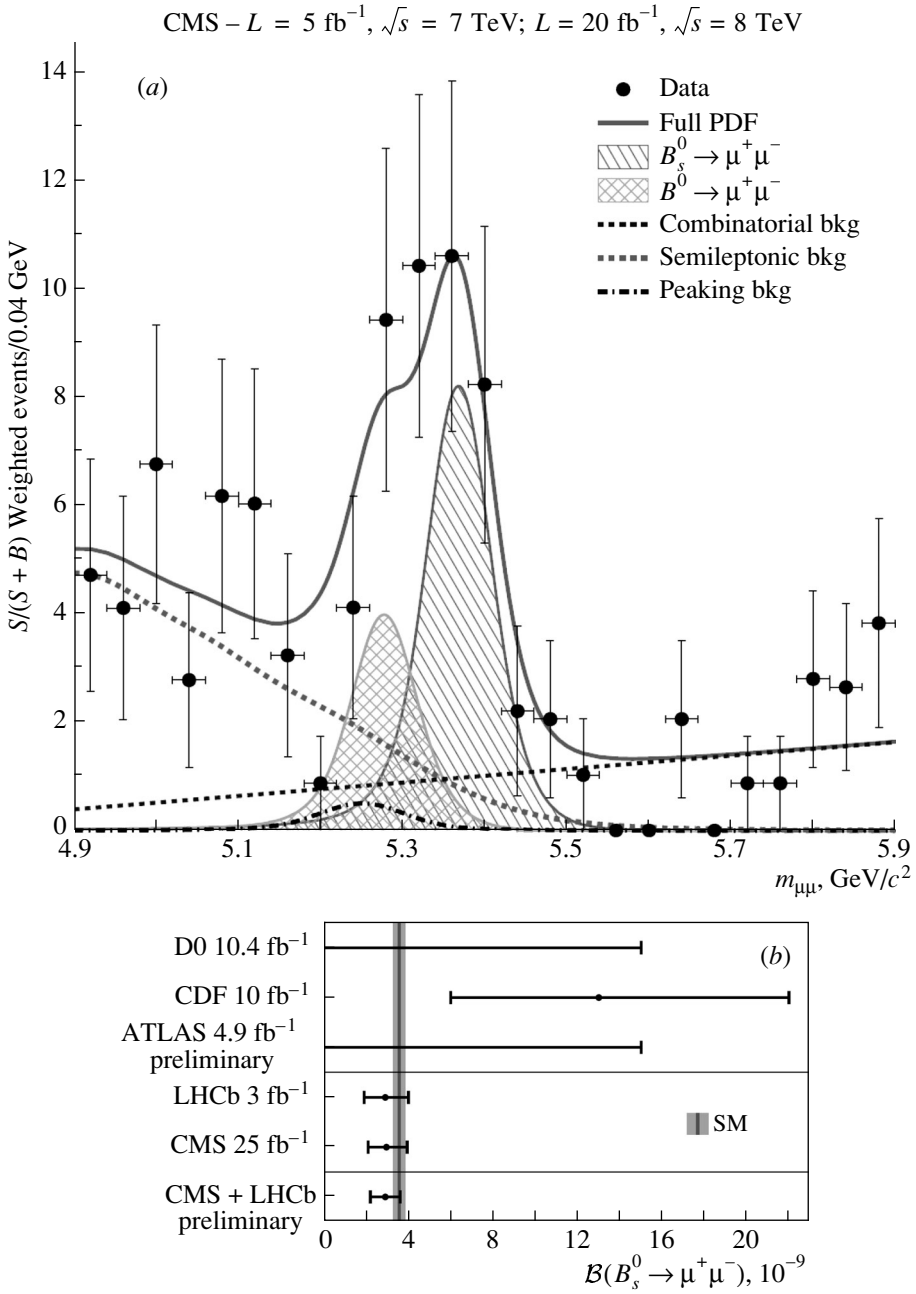

Fig. 3. (*a*) Invariant-mass distribution of dimuons. (*b*) Branching ratio for the decay $B_s \to \mu^+\mu^-$ according to measurements in various experiments.

1.1×10^{-9} at a 95% confidence level (C.L.), and there is agreement with the Standard Model once again.

By combining data of the CMS and LHCb experiments, it became possible to improve the precision of the measurements: $\mathcal{B}(B_s \to \mu^+\mu^-) = (2.9 \pm 0.7) \times 10^{-9}$ and $\mathcal{B}(B_0 \to \mu^+\mu^-) = (3.6^{+1.6}_{-1.4}) \times 10^{-10}$ [32]. Thus, the whole set of experimental data leaves virtually no chance for observing new physics in studying these rare decays (see Fig. 3*b*).

3. DISCOVERY OF THE HIGGS BOSON AND INVESTIGATION OF ITS PROPERTIES

The Standard Model predicts a short-lived Higgs boson decaying to other well-known particles. The CMS experiment explored five basic channels of Higgs boson decays: three channels of decay to a boson pair ($\gamma\gamma$, ZZ, or WW) and two channels of decay to two fermions ($b\bar{b}$ or $\tau\bar{\tau}$). In searches for a

Higgs boson of mass 125 GeV/c^2, the $\gamma\gamma$, ZZ, and WW channels have nearly the same potential. By and large, they are more sensitive than channels of decay to a $b\bar{b}$ or $\tau\bar{\tau}$ pair.

For the first time, a statistically significant excess of a signal above the Standard Model background was found in 2012 by the CMS Collaboration in analyzing a combined sample of data from the 2011 and 2012 runs in which the integrated luminosity was, respectively, 5.1 and 5.3 fb^{-1} [33]. In a simultaneous analysis of data on all five channels, the statistical significance of the excess of the signal above the background level was 4.9σ. A simultaneous analysis of data on the two most sensitive channels ensuring a high precision ($\gamma\gamma$ and ZZ) yielded a 5.0σ statistical significance of the observed effect. A unification of all data accumulated over two years made it possible to improve substantially the sensitivity of the analysis. A full list of the results concerning the discovery of the Higgs boson and the investigation of its properties is presented in [34].

3.1. Observation of a New Boson

The $\gamma\gamma$ and ZZ channels are of crucial importance since they make it possible to measure the mass of the new particle to a high degree of precision. In the $\gamma\gamma$ channel, the mass is determined from the energy and directions of motion measured for two high-energy photons by a crystalline electromagnetic calorimeter of the CMS detector. It the ZZ channel, the mass is determined from the decay of the Z-boson pair to two dielectrons, two dimuons, or a dielectron and a dimuon. They are measured by the inner tracker, electromagnetic calorimeter, and muon chambers. The mass resolution in the $\gamma\gamma$ and ZZ channels is not poorer than 1 to 2% [35]. The observation of two photons in the final state indicates that the new particle is a boson rather than a fermion and that its spin must not be 1. Figure 4*a* shows the mass distribution of four-lepton events featuring two dielectrons, two dimuons, or a dielectron and a dimuon. With allowance for their angular features, the excess of the number of events above the background level at mass values around 125 GeV/c^2 is 7.1σ [36]. The mass distribution of a diphoton is shown in Fig. 4*b*. It exhibits an excess of the number of events above the background level at mass values around 125 GeV/c^2, the statistical significance of this enhancement being 3.2σ [37].

The WW channel is more complicated. Each W boson is determined by its decay to an electron and a neutrino or a muon and a neutrino. The neutrino traversing the CMS detector remains undetected; therefore, the Higgs boson predicted by the Standard Model manifests itself as an enhancement of the number of events in a broad mass range with a statistical significance of 4.0σ [38] rather than as a narrow peak. The mass resolution in this channel is 20%.

Of particular interest for obtaining deeper insight into the nature of the discovered boson is the observation of its decays to a fermion pair ($b\bar{b}$ and $\tau\bar{\tau}$). The $b\bar{b}$ channel is marred by a heavy background from Standard Model processes; therefore, events in which a Higgs boson is produced together with W or Z boson decaying to electrons or muons are used in the analysis. The $\tau\bar{\tau}$ channel is measured by τ decays to electrons, muons, and hadrons. The mass resolution in the $b\bar{b}$ and $\tau\bar{\tau}$ channels is 10% and 15%, respectively. A data analysis based on the whole sample accumulated throughout the runs of 2011 and 2012 permitted revealing a peak in the $\tau\bar{\tau}$ and $b\bar{b}$ spectra at a level of 3.2σ [39] for the former and at a level of 2.1σ for the latter [40]. The statistical significance of the detection of fermionic decay modes in the simultaneous analysis of the two decay processes in question amounts to 3.8σ.

It is of paramount importance to test the hypothesis of extra scalar resonances—for example, extra Higgs bosons in models featuring an extended Higgs sector. At the present time, the CMS experimental data are quite sufficient for completely excluding their existence at a 95% C.L. in the mass range of 128–600 GeV/c^2 in the WW decay channel and in the mass range of 200–1000 GeV/c^2 in the ZZ decay channel [41]. Also, experiments have so far revealed no piece of evidence of the occurrence of rare and exotic (beyond the Standard Model) Higgs boson decays—for example, decays to a dimuon and so-called invisible decays in which final-state decay products do not contain Standard Model particles, which could be recorded by detecting systems, such as decays to four neutrinos, lightest stable supersymmetric particles (LSP), and dark-matter candidates (say, weakly interacting massive particles or WIMPs) [42].

3.2. Properties of the Higgs Boson

Two channels characterized by the highest mass resolution ($\gamma\gamma$ and ZZ) were used to measure the mass of the new boson. The mass of this new particle was determined without making any assumption on the decay-mode branching ratios. At the present time, it is $125.7 \pm 0.3(\text{stat.}) \pm 0.3(\text{syst.})$ GeV/c^2 [35]. In all five channels where a signal from the new particle in question was detected, the measured probability for the production of the new particle (σ_{DAT}) agrees with the value predicted by the Standard Model for

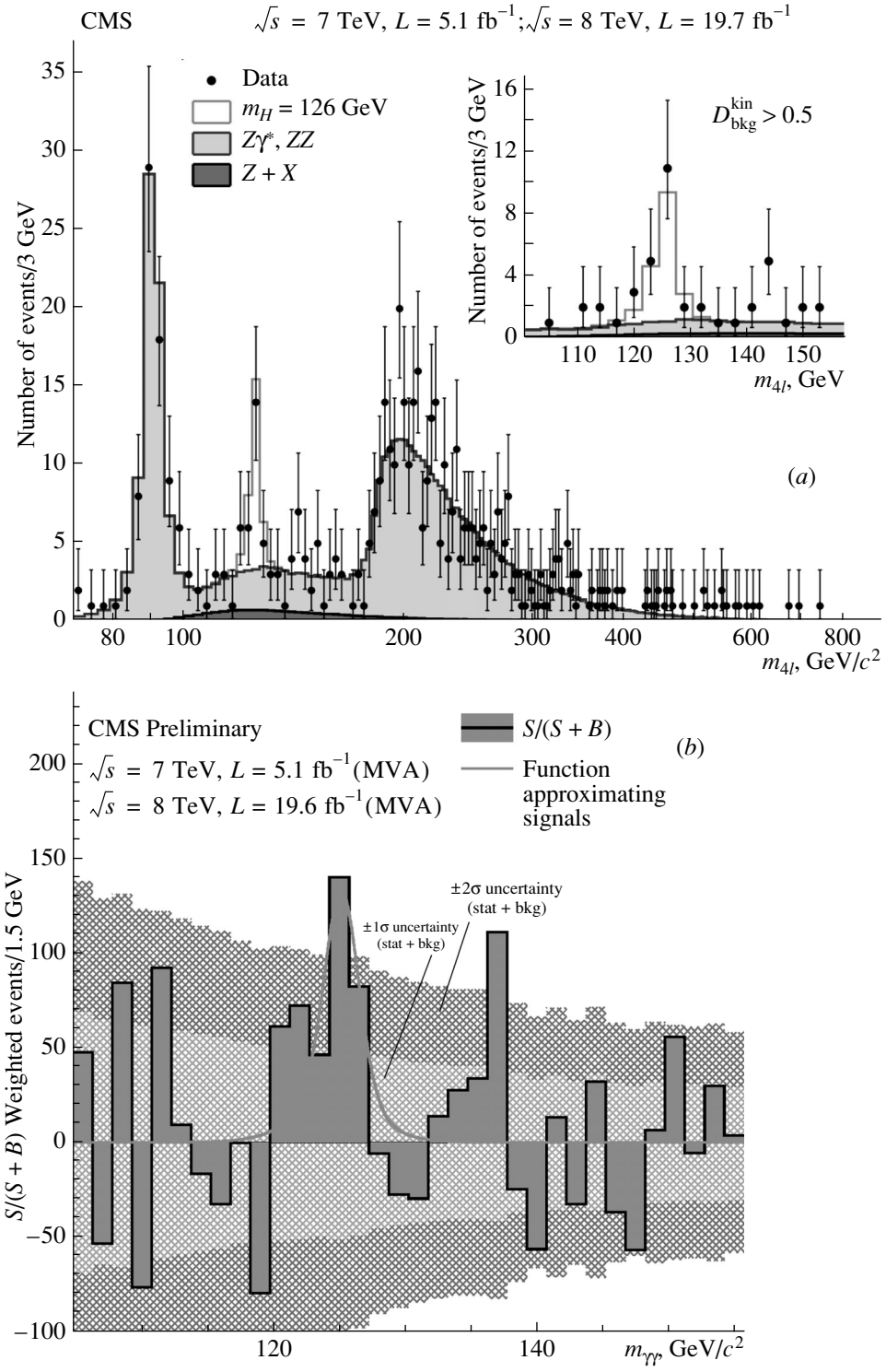

Fig. 4. Invariant-mass distribution of (*a*) four leptons [36] and (*b*) a diphoton [37].

the Higgs boson production probability (σ_{SM})—see Fig. 5*a*. Their ratio is referred to as the signal intensity and is denoted by μ. On the basis of the results of measurements for all five channels, the signal intensity is $\mu = \sigma_{\text{DAT}}/\sigma_{\text{SM}} = 0.80 \pm 0.14$ at the mass value of $m_H = 125.7$ GeV/c^2. The measured values of the coupling constants are also compatible with the Standard Model values of the Higgs boson

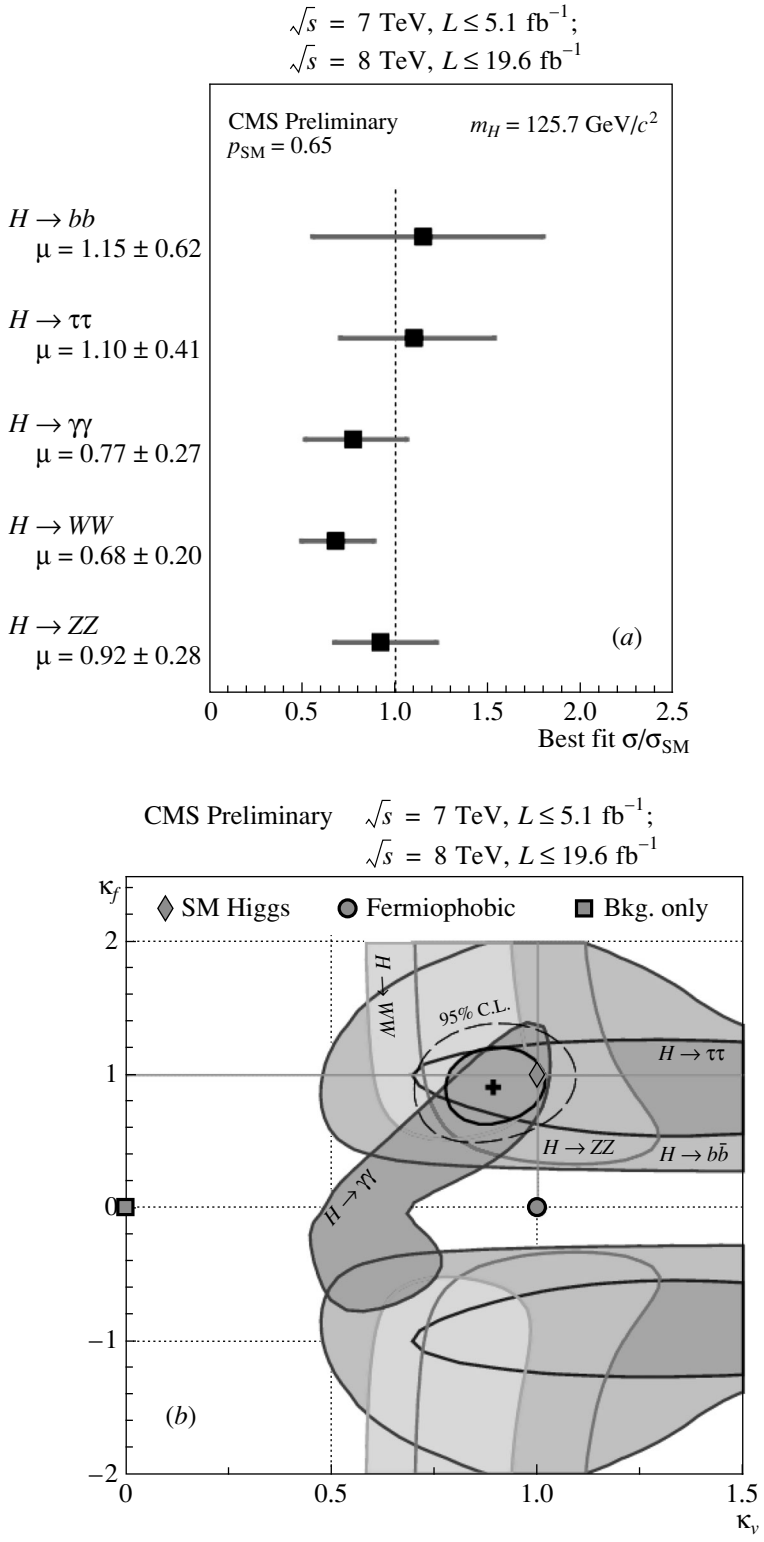

Fig. 5. (*a*) Signal intensity. (*b*) Admissible values of the vector and fermionic coupling constants.

coupling constants (see Fig. 5*b*). The hypothesis of a fermiofobic Higgs boson (that is, a Higgs boson not decaying to fermions) can also be excluded on the basis of the results obtained thus far.

In order to study the spin structure of the boson in question, use was made of so-called hypothesis separators, which are a combination of likelihood functions for competing hypotheses—that is,

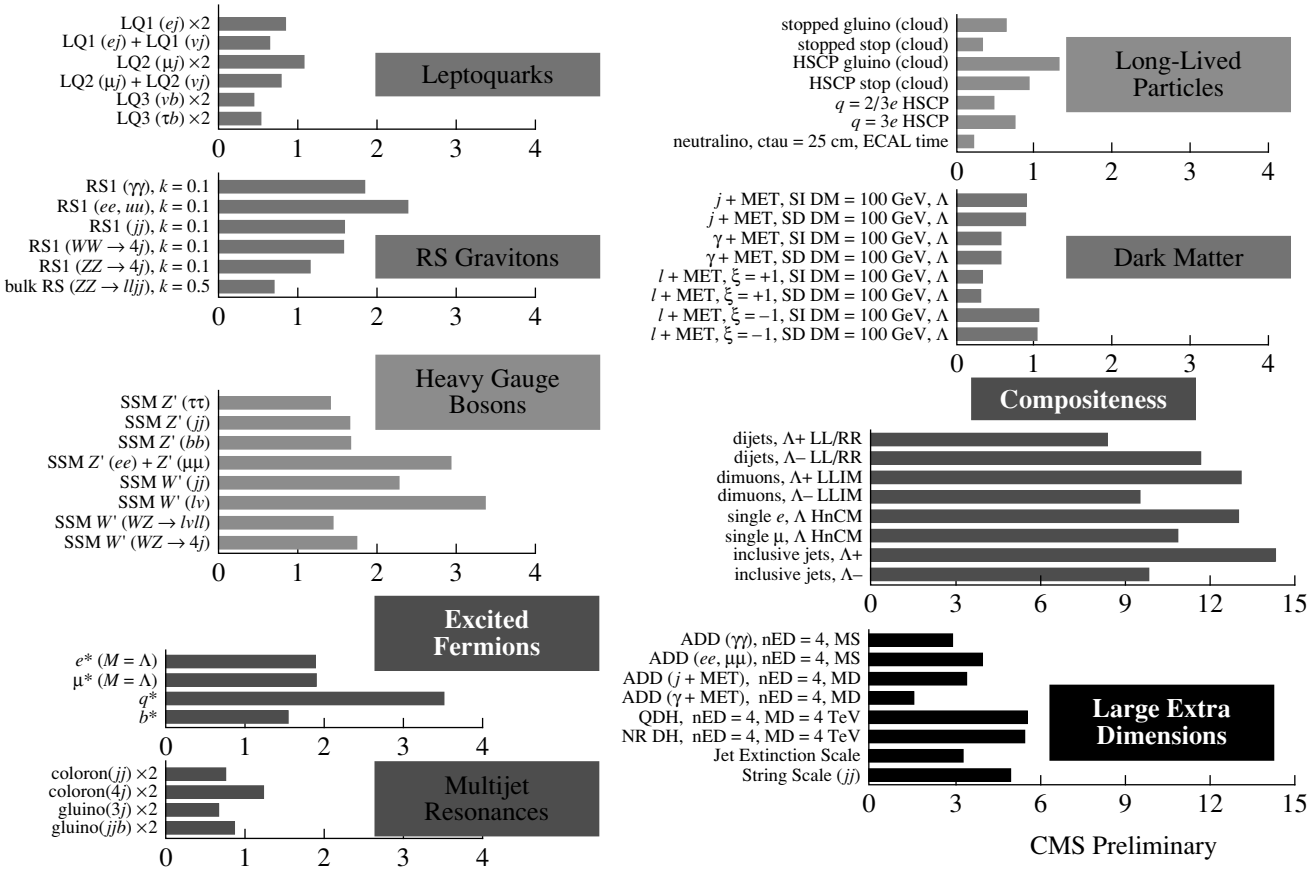

Fig. 6. Compendium of limits on the masses of hypothetical particles (in TeV/c^2 units).

the probability-density distributions for angular and mass variables of decay products under the assumption of various spins J and parities P. More than ten combinations of possible values of J and P were tested on the basis of data on ZZ decay to four leptons. These combinations corresponded to various pseudoscalar particles ($J^P = 0^-, \dots$), tensor particles ($J^P = 2^-, 2^+, \dots$), and even vector particles ($J^P = 1^-$ and 1^+), despite the fact that the observation of the $\gamma\gamma$ decay forbids the last option according to the Landau–Yang theorem. All combinations other than that which corresponds to the hypothesis of the Standard Model Higgs boson ($J^P = 0^+$) were rejected at a high statistical confidence level [36]. The results of the respective analysis for the $WW \to l\nu l\nu$ and $\gamma\gamma$ channels also rule out hypotheses not consistent with $J^P = 0^+$ [38, 43].

4. SEARCHES FOR SIGNALS FROM NEW PHYSICS BEYOND THE STANDARD MODEL

The CMS research program aimed at unearthing new physics beyond the Standard Model is a large-scale searching experiment devoted to discovering expected deviations from Standard Model predictions in various channels [3, 4]. The CMS Collaboration has been performing searches for signals from new physics objects and phenomena predicted by supersymmetric models, models featuring an extended gauge sector, scenarios of low-energy gravity, technicolor models, and many other theories. As observables, one employs various features of the production of Standard Model particles, including (i) heavy resonance states and nonresonance signals in the spectra of dimuons, dijets, diphotons, top-quark pairs, and gauge-boson pairs in searches for new heavy gauge bosons (Z'), Kaluza–Klein excited graviton states, technicolor particles, and so on and (ii) the single production of particles (jets, photons, leptons) that is accompanied by a large fraction of missed transverse energy [a deviation from Standard Model predictions in the behavior of such signals may be indicative of the existence of a new heavy charged gauge boson (W'), extra spatial dimensions, or weakly interacting dark-matter particles (WIMPs, for example)].

(iii) Further, measurement of the total scalar transverse momentum of particles originating from

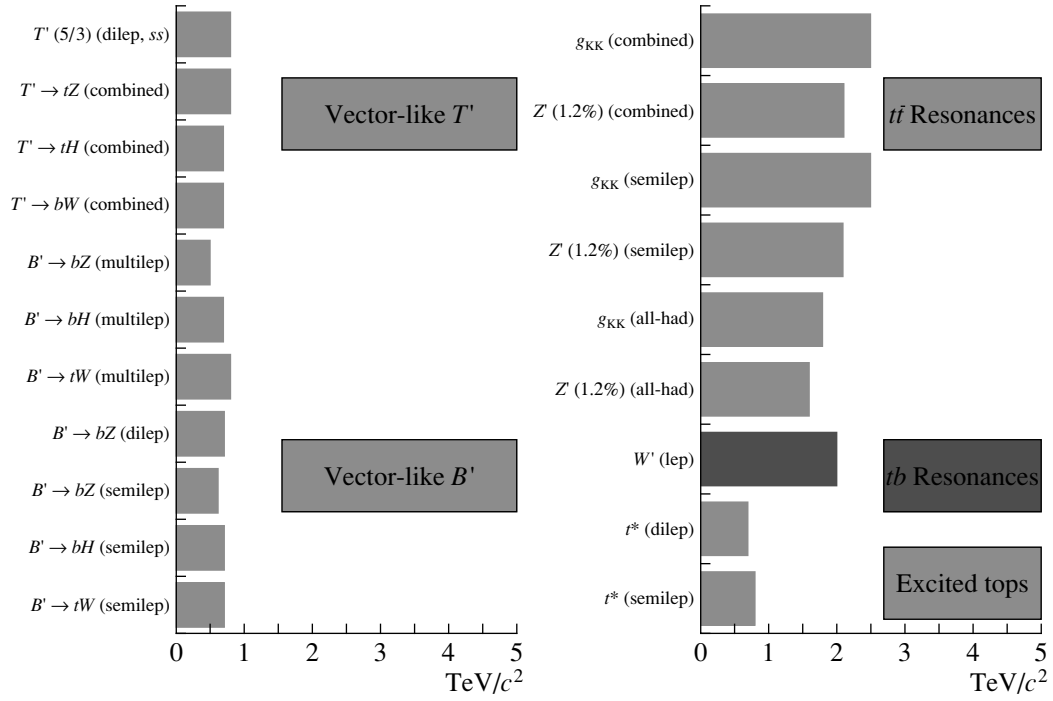

Fig. 7. Compendium of limits on the masses of new-physics particles in channels featuring b and t particles and on the masses of fourth-generation particles.

multiparticle-production processes is used in searches for microscopic black holes and leptoquarks.

(iv) The associated production of different particles (leptons and jets or leptons belonging to different generations) may be a signal from fourth-generation particles.

(v) As a rule, searches for supersymmetric particles are performed on the basis of measurements of sequential decays involving Standard Model particles or a missing energy in the final state.

No deviation of experimental data from Standard Model predictions have been found to date. Limits were set on the parameters of various theoretical models—for example, on the masses of new particles, fundamental energy scales, coupling constants, and cross sections for the production of new particles. A compendium of limits on the masses of hypothetical particles is given in Fig. 6 [44]. The list of limits obtained to date for the masses of new-physics particles in the channels featuring b and t quarks and for the masses fourth-generation particles [45] is presented in Fig. 7 in a tabular form.

Data obtained by the CMS Collaboration exclude at a 95% C.L. new neutral gauge bosons (Z') of mass below 2600 to 2950 GeV/c^2, the specific value of this limit being dependent on the coupling constants in the extended gauge sector; in the RS1 scenario of the Randall–Sundrum model, these data exclude the Kaluza–Klein graviton of mass below 2030 to 2390 GeV/c^2, the specific value here being dependent on the ratio of the radius of curvature of the multidimensional space being considered to the Planck fundamental scale. In models of the Arkani-Hamed–Dimopoulos–Dvali (ADD) type, the multidimensional fundamental scale is constrained from below by a value falling within the range of 3–5.1 TeV and depending on the number of extra spatial dimensions. The effective contact-interaction scale Λ in composite models and in WIMP (candidates for dark-matter particles) models is constrained by values in the range of 8–14 TeV and by about 1 TeV, respectively. Also, limits were set on the masses of leptoquarks belonging to three generations, excited fermions, multijet resonances (see Fig. 6) and fourth-generation particles (see Fig. 7).

The concept of supersymmetry is one of the most popular extensions of the Standard Model. The predicted spectrum of supersymmetric particles is an object of searches at the LHC. An attempt at discovering signals from such particles—for example, in cascade-decay chains—with the CMS detector was undertaken in course of the first run at the LHC. In particular, the range of possible stop-quark (supersymmetric partner $\tilde{t}$ of the top quark) masses was studied in the decays $\tilde{t} \to t\tilde{\chi}^0$ and $\tilde{t} \to b\tilde{\chi}^+$, this range being limited from below by the top-quark mass. The search for $\tilde{b}$ was performed in the decay channels $\tilde{b} \to b\tilde{\chi}^0$, $\tilde{b} \to tW\tilde{\chi}^0$, and $\tilde{b} \to bZ\tilde{\chi}^0$. The

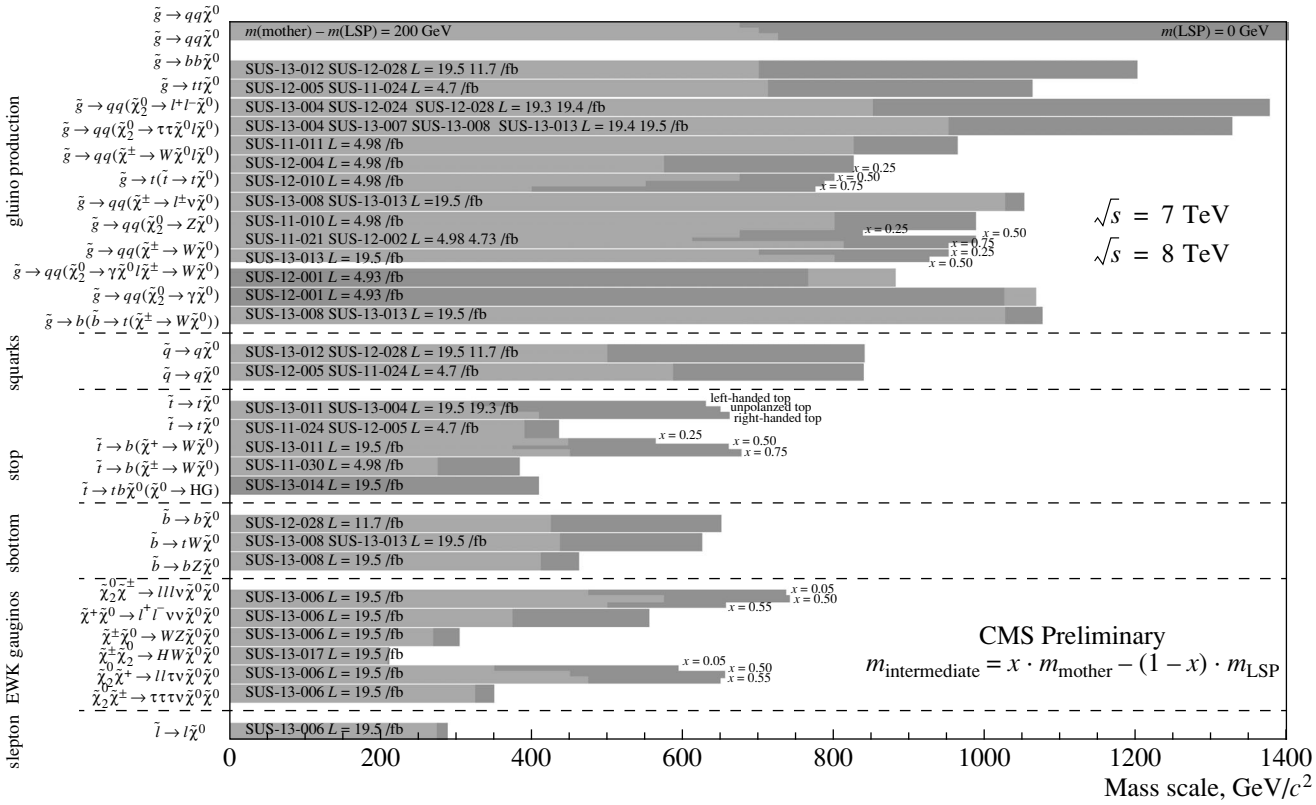

Fig. 8. Compendium of limits on the masses of supersymmetric particles.

resulting limits on the $\tilde{t}$ and $\tilde{b}$ masses fell within the ranges of 200–710 and 320–610 GeV/c^2, respectively, at neutralino-mass values below 200 GeV/c^2 (see Fig. 8) [46]. The limits on the gluino, squark, and chargino masses proved to be between 1.1 to 1.3 TeV/c^2, 0.78 TeV/c^2, and 500 GeV/c^2, respectively.

5. HEAVY-ION PHYSICS

Investigations into heavy-ion physics in the CMS experiment [47] were performed in 2010 and 2011 in colliding beams of lead nuclei at the c.m. collision energy of $\sqrt{s_{NN}} = 2.76$ TeV. The integrated luminosity $\mathcal{L}_{\text{int}}$ in these runs was 10 and 155 μb^{-1}, respectively. A run with proton and lead-ion beams was conducted in 2012 at $\sqrt{s_{NN}} = 5.02$ TeV and $\mathcal{L}_{\text{int}} = 1\ \mu\text{b}^{-1}$.

Unique measurements of the disbalance of the transverse momentum of leading jets in relation to secondary jets were performed in PbPb collisions [48]. This confirmed the effect of jet quenching in dense nuclear matter. The observations also included the sequential suppression of the production of $\Upsilon(2S)$ and $\Upsilon(3S)$ resonances in relation to their yield in pp collisions [49] and the suppression of directly and indirectly produced J/ψ and $\Upsilon(1S)$ particles [50]; the suppression of high-p_T charged particles was studied [51]. The cross section for the production of the Z gauge boson in nucleus–nucleus collisions was measured for the first time [52]. In 2012, long-range angular correlations (so-called ridge effect) were observed in high-multiplicity events of proton–nucleus collisions [53]; earlier, this effect was first observed in pp collisions in 2010 [54].

6. CONCLUSIONS

New unique data on interactions of Standard Model particles at record energies were obtained in the course of the first run of LHC operation. The Higgs boson was discovered, and investigation of its properties was initiated. Long-range correlations were observed in proton–proton and proton–nucleus interactions. Measurements were performed for Standard Model processes, including rare and previously unobserved (associated tW production) ones, and for the decay process $B_s \to \mu^+\mu^-$. This permitted refining some parameters of the Standard Mode and setting limits on the parameters of some theoretical models beyond the Standard Model—for

example, on the masses of new particles, on the fundamental energy scales, on the coupling constants, and on the cross sections for the production of new particles. To date, the CMS Collaboration published more than 300 articles. All results of the CMS experiment are listed in [55].

The results of the CMS experiment that are discussed in the present article agree with the results of the ATLAS experiment [56], which is the other multipurpose experiment at the Large Hadron Collider.

ACKNOWLEDGMENTS

I am grateful A.V. Lanyov, M.V. Savina, and other participants of the CMS experiment for enlightening comments and discussions in the course of the preparation of this article for publication. This work was supported by the Ministry of Education and Science of Russian Federation under an agreement (no. 14.610.21.0004) of October 14, 2014 (ID no. RMFEFI61014X0004).

REFERENCES

1. CMS Collab. (S. Chatrchyan et al.), JINST **3**, S08004 (2008).
2. V. A. Rubakov, Phys. Usp. **55**, 949 (2012).
3. CMS Collab. (G. L. Bayatian et al.), J. Phys. G **34**, 995 (2007).
4. I. A. Golutvin, V. V. Palichik, M. V. Savina, and S. V. Shmatov, Phys. At. Nucl. **70**, 56 (2007); S. V. Shmatov, Phys. At. Nucl. **74**, 490 (2011); **76**, 1106 (2013); M. V. Savina, Phys. At. Nucl. **74**, 496 (2011); **76**, 1090 (2013).
5. CMS Collab. (S. Chatrchyan et al.), Phys. Rev. Lett. **105**, 022002 (2010), arXiv: 1005.3299 [hep-ex]; J. High Energy Phys. **1101**, 079 (2011), arXiv: 1011.5531 [hep-ex].
6. CMS Collab. (S. Chatrchyan et al.), Phys. Rev. D **87**, 112002 (2013), arXiv: 1212.6660 [hep-ex].
7. CMS Collab. (S. Chatrchyan et al.), Phys. Lett. B **700**, 187 (2011), arXiv: 1104.1693 [hep-ex].
8. CMS Collab. (S. Chatrchyan et al.), Phys. Rev. Lett. **106**, 201804 (2011), arXiv: 1102.2020 [hep-ex].
9. CMS Collab. (S. Chatrchyan et al.), Phys. Lett. B **702**, 336 (2011), arXiv: 1106.0647 [hep-ex]; Eur. Phys. J. C **73**, 2604 (2013), arXiv: 1304.7498 [hep-ex].
10. CMS Collab. (S. Chatrchyan et al.), CMS-SMP-12-028, CERN-PH-EP-2014-238, arXiv: 1410.6765 [hep-ex].
11. CMS Collab. (S. Chatrchyan et al.), J. High Energy Phys. **1110**, 132 (2011), arXiv: 1107.4789 [hep-ex].
12. CMS Collab. (S. Chatrchyan et al.), Phys. Rev. Lett. **112**, 191802 (2014), arXiv: 1402.0923 [hep-ex].
13. CMS Collab. (S. Chatrchyan et al.), J. High Energy Phys. **1201**, 010 (2012), arXiv: 1110.3226 [hep-ex].
14. CMS Collab. (S. Chatrchyan et al.), CMS-PAS-EWK-11-010; Phys. Lett. B **701**, 535 (2011), arXiv: 1105.2758 [hep-ex].
15. CMS Collab. (S. Chatrchyan et al.), Phys. Lett. B **721**, 190 (2013), arXiv: 1301.4698 [hep-ex].
16. CMS Collab. (S. Chatrchyan et al.), J. High Energy Phys. **1312**, 30 (2013), arXiv: 1310.7291 [hep-ex]; J. High Energy Phys. **1110**, 007 (2011), arXiv: 1108.0566 [hep-ex].
17. CMS Collab. (S. Chatrchyan et al.), Phys. Lett. B **718**, 752 (2013), arXiv: 1207.3973 [hep-ex].
18. I. N. Gorbunov and S. V. Shmatov, Phys. At. Nucl. **76**, 1100 (2013); Phys. Part. Nucl. **45**, 211 (2014).
19. CMS Collab. (S. Chatrchyan et al.), Phys. Rev. D **84**, 112002 (2011), arXiv: 1110.2682 [hep-ex].
20. CMS Collab. (S. Chatrchyan et al.), CMS-PAS-TOP-12-001.
21. The Tevatron Electroweak Working Group, arXiv: 1107.5255v3 [hep-ex].
22. CMS Collab. (S. Chatrchyan et al.), Phys. Lett. B **695**, 424 (2011), arXiv: 1010.5994 [hep-ex].
23. CMS Collab. (S. Chatrchyan et al.), J. High Energy Phys. **1402**, 024 (2014), arXiv: 1312.7582 [hep-ex].
24. CMS Collab. (S. Chatrchyan et al.), J. High Energy Phys. **1212**, 035 (2012), arXiv: 1209.4533 [hep-ex].
25. CMS Collab. (S. Chatrchyan et al.), CMS-PAS-TOP-12-011.
26. CMS Collab. (S. Chatrchyan et al.), Phys. Rev. Lett. **110**, 022003 (2013), arXiv: 1209.3489 [hep-ex].
27. CMS Collab. (S. Chatrchyan et al.), CMS-PAS-TOP-12-016.
28. CMS Collab. (S. Chatrchyan et al.), CMS-PAS-TOP-12-004.
29. CMS Collab. (S. Chatrchyan et al.), Phys. Rev. Lett. **112**, 231802 (2014), arXiv: 1401.2942 [hep-ex].
30. LHCb Collab. (R. Aaij et al.), Phys. Rev. Lett. **110**, 021801 (2013), arXiv: 1211.2674 [hep-ex].
31. CMS Collab. (S. Chatrchyan et al.), Phys. Rev. Lett. **111**, 101804 (2013), arXiv: 1307.5025 [hep-ex].
32. CMS and LHCb Collab., CMS-PAS-BPH-13-007; LHCb-CONF-2013-012.
33. CMS Collab. (S. Chatrchyan et al.), Phys. Lett. B **716**, 30 (2012), arXiv: 1207.7235 [hep-ex].
34. https://twiki.cern.ch/twiki/bin/view/CMSPublic/PhysicsResultsHIG
35. CMS Collab. (S. Chatrchyan et al.), CMS-PAS-HIG-13-005.
36. CMS Collab. (S. Chatrchyan et al.), Phys. Rev. D **89**, 092007 (2014), arXiv: 1312.5353 [hep-ex].
37. CMS Collab. (S. Chatrchyan et al.), CMS-PAS-HIG-13-001.

38. CMS Collab. (S. Chatrchyan et al.), J. High Energy Phys. **1401**, 096 (2014), arXiv: 1312.1129 [hep-ex].
39. CMS Collab. (S. Chatrchyan et al.), J. High Energy Phys. **1405**, 104 (2014), arXiv: 1401.5041 [hep-ex].
40. CMS Collab. (S. Chatrchyan et al.), Phys. Rev. D **89**, 012003 (2014), arXiv: 1310.3687 [hep-ex].
41. CMS Collab. (S. Chatrchyan et al.), CMS-PAS-HIG-13-014.
42. CMS Collab. (S. Chatrchyan et al.), CMS-PAS-HIG-13-018; CMS-PAS-HIG-13-013; CMS-PAS-HIG-13-028.
43. CMS Collab. (S. Chatrchyan et al.), CMS-PAS-HIG-13-016.
44. https://twiki.cern.ch/twiki/bin/view/CMSPublic/PhysicsResultsEXO
45. https://twiki.cern.ch/twiki/bin/view/CMSPublic/PhysicsResultsB2G
46. https://twiki.cern.ch/twiki/bin/view/CMSPublic/PhysicsResultsSUS
47. CMS Collab. (G. L. Bayatian et al.), J. Phys. G **34**, 995 (2007).
48. CMS Collab. (S. Chatrchyan et al.), Phys. Rev. C **84**, 024906 (2011), arXiv: 1102.1957 [nucl-ex].
49. CMS Collab. (S. Chatrchyan et al.), Phys. Rev. Lett. **109**, 222301 (2012), arXiv: 1208.2826 [nucl-ex]; Phys. Rev. Lett. **107**, 052302 (2011), arXiv: 1105.4894 [nucl-ex].
50. CMS Collab. (S. Chatrchyan et al.), J. High Energy Phys. **1205**, 063 (2012), arXiv: 1201.5069 [nucl-ex].
51. CMS Collab. (S. Chatrchyan et al.), Eur. Phys. J. C **72**, 1945 (2012), arXiv: 1202.2554 [nucl-ex].
52. CMS Collab. (S. Chatrchyan et al.), CMS-PAS-HIN-12-008.
53. CMS Collab. (S. Chatrchyan et al.), Phys. Lett. B **718**, 795 (2013), arXiv: 1210.5482 [nucl-ex].
54. CMS Collab. (S. Chatrchyan et al.), J. High Energy Phys. **1009**, 091 (2010), arXiv: 1009.4122 [nucl-ex].
55. https://twiki.cern.ch/twiki/bin/view/CMSPublic/PhysicsResults
56. https://twiki.cern.ch/twiki/bin/view/AtlasPublic